BNL-96388-2011-JA

# *OBSERVATIONAL-BASED EVALUATION OF NWP REANALYSES IN MODELING CLOUD PROPERTIES OVER THE SOUTHERN GREAT PLAINS*

Wei Wu[1*], Yangang Liu[1] and Alan K. Betts[2]

[1]Atmospheric Sciences Division, Brookhaven National Laboratory, Upton, NY 11973, USA
[2]Atmospheric Research, Pittsford, VT 05763, USA
*Corresponding author: Wei Wu, Atmospheric Sciences Division, Brookhaven National Laboratory, 75 Rutherford Dr., Bldg. 815E, Upton, NY 11973; Email: wwu@bnl.gov

Submitted to
*J. Geophys. Res.*

October 2011

**Atmospheric Sciences Division/Environmental Sciences Dept.**

**Brookhaven National Laboratory**

**U.S. Department of Energy
Office of Science**

Notice: This manuscript has been authored by employees of Brookhaven Science Associates, LLC under Contract No. DE-AC02-98CH10886 with the U.S. Department of Energy. The publisher by accepting the manuscript for publication acknowledges that the United States Government retains a non-exclusive, paid-up, irrevocable, world-wide license to publish or reproduce the published form of this manuscript, or allow others to do so, for United States Government purposes.

This preprint is intended for publication in a journal or proceedings. Since changes may be made before publication, it may not be cited or reproduced without the author's permission.

## DISCLAIMER

This report was prepared as an account of work sponsored by an agency of the United States Government. Neither the United States Government nor any agency thereof, nor any of their employees, nor any of their contractors, subcontractors, or their employees, makes any warranty, express or implied, or assumes any legal liability or responsibility for the accuracy, completeness, or any third party's use or the results of such use of any information, apparatus, product, or process disclosed, or represents that its use would not infringe privately owned rights. Reference herein to any specific commercial product, process, or service by trade name, trademark, manufacturer, or otherwise, does not necessarily constitute or imply its endorsement, recommendation, or favoring by the United States Government or any agency thereof or its contractors or subcontractors. The views and opinions of authors expressed herein do not necessarily state or reflect those of the United States Government or any agency thereof.

## Abstract

This study evaluates three major Numerical-Weather-Prediction (NWP) reanalyses (ERA-Interim, NCEP/NCAR Reanalysis, and NCEP/DOE Reanalysis) in modeling surface relative shortwave cloud forcing, cloud fraction, and cloud albedo. The observations used for this evaluation are surface-based continuous measurements of the US Atmospheric Radiation Measurement (ARM) program from 03/25/1997 to 12/31/2008 over the Southern Great Plains (SGP) site. These cloud properties from the reanalyses are evaluated at multiple temporal scales. Like the observations, all the reanalyses show a strong annual cycle, and relatively weak diurnal or inter-annual variations of the cloud properties. The reanalyses exhibit significant underestimation on the cloud properties, and the model biases of the cloud properties are linearly linked to one another. Further analysis reveals that the model biases of the cloud properties exhibit quasi-linear relationships to the model biases of near-surface relative humidity (and temperature for ERA-Interim). A combined statistical analysis using the technique of Taylor diagrams and a newly developed metric "Relative Euclidean Distance" indicates that ERA-Interim (NCEP/NCAR Reanalysis) has the best (worst) overall performance among the three reanalyses.

## 1. Introduction

Climate prediction depends on modeling, so there is a pressing need to quantify model uncertainties and reduce model biases. Among numerous model uncertainties, the representation of clouds and associated radiative processes has been recognized as one of the most uncertain factors in global climate models (GCMs), which limit the accuracy of climate prediction [IPCC, 2007]. As a consequence, model evaluations to identify deficiencies in the parameterization of clouds and associated radiative processes remain a field of intensive research.

To address this long-standing climate issue, the US Department of Energy's (DOE's) Earth System Modeling program funded a new model evaluation project in 2009: the FAst-physics System TEstbed and Research (FASTER) project. The main thrust of this multi-institutional project is to accelerate the evaluation and improvement of the parameterizations of cloud-related fast processes in large-scale climate models, by using various long-term observations from the DOE's Atmospheric Radiation Measurement (ARM) program and satellites collected over the ARM sites. This paper is an initial evaluation of the representation of clouds and associate radiative processes in three major Numerical-Weather-Prediction (NWP) reanalyses.

As representations of the state of the atmosphere, reanalyses are generated via a state-of-art analysis and forecast system assimilating data from a wide variety of observations including ships, satellites, ground stations and radar. The long-term, consistent global distributions of reanalyses make them particularly valuable in climate research, and they have been widely used as a base-line in studying global climate change and climate modeling [e.g., Lu et al., 2005; Anderson et al., 2008; Haimberger et al., 2008; Betts et al., 2009; Simmons et al., 2010; Rye et al., 2010]. Nonetheless, despite several distinct advantages over more traditional climate datasets, reanalyses have been found contaminated by time-varying biases, suggesting a limitation for characterizing long-term

climate trends [e.g., Thorne and Vose, 2010; Dee et al., 2011]. Furthermore, cloud data are not directly assimilated into reanalyses. Instead, cloud-related properties of reanalyses are computed from model parameterizations, and often have biases which must be evaluated, similar to those in GCMs. For these reasons, observational-based evaluations of widely used reanalyses are crucial to not only this FASTER project, but also the whole community of climate researchers.

In this study we evaluate three major NWP reanalyses in modeling surface relative shortwave cloud forcing (see section 2.3.1), cloud fraction, and cloud albedo. We use decade-long (1997 to 2008) surface-based continuous ARM value-added products (VAP) over the Southern Great Plains (SGP) Central Facility site as a standard for this evaluation.

We first evaluate the diurnal, annual and inter-annual variations of the cloud properties from the reanalyses. Then, we analyze the model biases of the cloud properties and their links to one another and to the common meteorological variables (i.e., temperature and relative humidity). Finally, the overall performance of the reanalyses in modeling the cloud properties is evaluated. Section 2 briefly introduces the data and methods used. Section 3 shows the multiscale variations of the cloud properties. Section 4 analyzes model biases and their links. Section 5 evaluates the overall performance of the reanalyses. Section 6 summarizes this study.

## 2. Data and Methods

This section briefly introduces the data (e.g., observations and reanalyses) and methods used in this study. Note that this study only evaluates daytime cloud properties, since shortwave radiation observations are used.

## 2.1 Observations

The observations used are the high-resolution ARM VAP from well-calibrated surface-based continuous measurements of surface shortwave (SW) radiation flux and fractional sky cover ("cloud fraction" hereafter) over the SGP Central Facility (262.51$^{o}$E, 36.61$^{o}$N), generated by Long and his co-workers [Long and Ackerman, 2000; Long et al., 2006]. The VAP are based on the measurements collected by the Solar and Infrared Radiation System (SIRS) since 25 March 1997, and contains all the data needed for this evaluation. We use the 15-min datastreams of all-sky and clear-sky-fit surface downwelling SW fluxes and total cloud fraction from 03/25/1997 to 12/31/2008. Surface relative shortwave cloud forcing (SRCF) is calculated using the all-sky and clear-sky SW fluxes, and cloud albedo is calculated using both SRCF and cloud fraction. In addition, we also use the 30-min datastreams of 2m air temperature and relative humidity from the Surface Meteorological Observation System (SMOS) instruments from 04/01/2001 to 12/31/2008 for analyzing the links of the model biases of the cloud properties to those of near-surface meteorological conditions.

## 2.2 Reanalyses

The three major NWP reanalyses (i.e., ERA-Interim, NCEP/NCAR Reanalysis I, and NCEP/DOE Reanalysis II) are evaluated in this study. The abbreviations "ERA", "NCEP", and "NCAR" denote "European Centre for Medium-Range Weather Forecasts (ECMWF) global atmospheric reanalysis", "National Center for Environmental Prediction", and "National Center for Atmospheric Research", respectively. A brief introduction is given below.

### 2.2.1 ERA-Interim

ERA-Interim is an improved version of ECMWF's previous reanalysis ERA-40. It provides data from 1989 to present. This reanalysis was archived in a horizontal resolution of T255 spherical-harmonic representation for the basic dynamical fields or N128 reduced Gaussian grid with approximately uniform 79 km spacing for surface and other grid-point fields, with 60 vertical levels [Berrisford et al., 2009]. The global archive has 6-hourly time resolution, but for selected points, including the ARM SGP site, hourly data were archived which we use here. The major improvements in ERA-Interim include the representation of hydrological cycle, the quality of stratospheric circulation, and the handling of bias and changes in the observing system. One advantage of this reanalysis is its high spatial and temporal resolutions, better for studying regional diurnal variations. Detailed description about this reanalysis can be found at the ECMWF web site at http://www.ecmwf.int//research/era/do/get/ERA-Interim. We use hourly clear-sky surface net SW flux, and all-sky surface net and surface downwelling SW fluxes, total cloud cover, 2m air temperature and specific humidity, and surface pressure from 03/25/1997 to 12/31/2008. The hourly data are the outputs from the first 0-12 hour forecasts from twice-daily analysis. All the data used are from a Gaussian grid centered at (262.50 $^{o}$E, 36.84 $^{o}$N) over the ARM SGP site.

Note that, ERA-Interim hourly clear-sky surface downwelling SW flux ($SW_{dn}^{clear}$) is not available so it is calculated from Equation (1) using the available clear-sky surface net SW flux ($SW_{net}^{clear}$), all-sky surface downwelling SW flux ($SW_{dn}^{all}$) and all-sky surface net SW flux ($SW_{net}^{all}$),

$$SW_{dn}^{clear} = \frac{SW_{net}^{clear} \times SW_{dn}^{all}}{SW_{net}^{all}} \quad (1)$$

Equation (1) is derived based on Equation (2) in Betts et al. [2009] under the assumption that surface albedo is the same for clear-sky and cloudy-sky conditions. Here, several data points with "negative" or "spike" clear-sky surface downwelling SW flux are marked as "bad" data points and not included in further analysis.

Note also that, ERA-Interim hourly 2m relative humidity is not available so it is calculated using Equation (2) [i.e., Equation (3.62) in Peixoto and Oort, 1992],

$$\mathrm{rh} = \frac{q}{q_s} = \frac{pq}{0.622 e_s} \tag{2}$$

where rh, $q$, $q_s$, $p$, $e_s$, and $T$ represent relative humidity, specific humidity (kg/kg), saturation specific humidity (kg/kg), pressure of moist air (hPa), saturation vapor pressure (hPa), and temperature (K) of moist air. The saturation vapor pressure $e_s$ is calculated using Equation (3) of saturation vapor pressure, recommended by World Meteorological Organization (http://cires.colorado.edu/~voemel/vp.html),

$$\log_{10}(e_s) = 10.79574 \times \left(1 - \frac{273.16}{T}\right) - 5.02800 \times \log_{10}\left(\frac{T}{273.16}\right)$$

$$+ 1.50475 \times 10^{-4} \times \left(1 - 10^{-8.2969 \times \left(\frac{T}{273.16} - 1\right)}\right)$$

$$+ 0.42873 \times 10^{-3} \times \left(10^{4.76955 \times \left(1 - \frac{273.16}{T}\right)} - 1\right) + 0.78614 \tag{3}$$

### 2.2.2 NCEP/NCAR Reanalysis I

NCEP/NCAR Reanalysis I (R1 hereafter) [Kalnay et al. 1996; Kistler et al. 2001] provides data from 1948 to the present with 6-hour temporal resolution. The spatial resolution archived in this reanalysis is T62 Gaussian grid (~ 210 km), or 2.5$^{o}$ latitude x 2.5$^{o}$ longitude non-Gaussian grid, with 28 vertical levels. This reanalysis was generated via an analysis and forecast system to perform data assimilation using a wide variety of weather observations including ships, satellites, ground stations and radar. In this paper, we use 6-hourly clear-sky and all-sky surface downwelling SW flux, total cloud cover, 2m air temperature and near-surface (sigma level 995) relative humidity over the ARM SGP site from 03/25/1997 to 12/31/2008. All the data used are from a Gaussian grid centered at (262.50 $^{o}$ E, 37.14 $^{o}$ N) except the relative humidity data that are from a non-Gaussian grid centered at (262.50 $^{o}$ E, 37.50 $^{o}$ N). These data are downloaded from the NOAA's Physical Science Division web site at http://www.esrl.noaa.gov/psd/data/gridded/reanalysis/.

### 2.2.3 NCEP/DOE Reanalysis II

NCEP/DOE Reanalysis II (R2 hereafter) is a second version of R1. It covers data from 1979 to present, available at the same web site as R1. This reanalysis is believed to be an improved version of R1, with a number of errors fixed, updated parameterizations of physical processes (including a new SW radiation scheme which significantly reduced surface insolation by about 8%), and the addition of more observations [Kanamitsu et al. 2002]. Similarly, we use R2 6-hourly all-sky surface downwelling SW flux, total cloud cover, 2m air temperature and near-surface (1000 hPa) relative humidity over the ARM SGP site from 03/25/1997 to 12/31/2008. Since the archive does not provide R2 clear-sky surface downwelling SW flux, we estimate it by using R1 clear-sky surface

downwelling SW flux and the following expressions for the best fit to the available R2 all-sky surface downwelling SW flux,

$$SW_{dn}^{clear}(t,\mathrm{d};\mathrm{R2}) = SW_{dn}^{clear}(t,d;\mathrm{R1}) \times \left[0.85 + \frac{(0.92-0.85)d}{60}\right] \qquad (\text{for } d \le 60) \qquad (4\text{-}1)$$

$$SW_{dn}^{clear}(t,\mathrm{d};\mathrm{R2}) = SW_{dn}^{clear}(t,d;\mathrm{R1}) \times 0.92 \qquad (\text{for } 60 < d < 120 \text{ or } 220 < d < 280) \qquad (4\text{-}2)$$

$$SW_{dn}^{clear}(t,\mathrm{d};\mathrm{R2}) = SW_{dn}^{clear}(t,d;\mathrm{R1}) \times \left[0.92 + 0.02 \times \sin\frac{\pi(d-120)}{100}\right] \quad (\text{for } 120 \le d \le 220)) \quad (4\text{-}3)$$

$$SW_{dn}^{clear}(t,\mathrm{d};\mathrm{R2}) = SW_{dn}^{clear}(t,d;\mathrm{R1}) \times \left[0.92 - \frac{(0.92-0.85)(d-280)}{86}\right] \quad (\text{for } 280 < d \le 366) \quad (4\text{-}4)$$

where $SW_{dn}^{clear}(t,\mathrm{d};\mathrm{R1})/SW_{dn}^{clear}(t,\mathrm{d};\mathrm{R2})$ denotes R1/R2 6-hourly clear-sky surface downwelling SW flux, $t$ denotes 6-hourly time of a day, and $d$ denotes calendar day of a year. The estimated R2 6-hourly clear-sky surface downwelling SW flux is shown in Figure 1.

### 2.3 Methods

We will first briefly introduce the calculations of SRCF and cloud albedo. Then, we will give a detailed description of the procedures used for this study.

#### 2.3.1 SRCF

SRCF (also called "effective cloud albedo") was first proposed by Betts and Viterbo [2005] for quantifying the impact of the cloud field on the surface radiative budget over a southwest basin of the Amazon. It is a non-dimensional measure of surface SW cloud forcing ($F_{cld}$), defined as

$$\alpha_{cld}^{SRF} = -\frac{F_{cld}}{F_{clr}^{dn}} = 1 - \frac{F_{all}^{dn}}{F_{clr}^{dn}} \quad (5)$$

where $F_{all}^{dn}$ and $F_{clr}^{dn}$ denote all-sky and clear-sky surface downwelling SW fluxes, with positive values being indicative of downward fluxes. Based on Equation (5), we can calculate SRCF if all-sky and clear-sky surface downwelling SW fluxes are available.

Furthermore, Equation (5) indicates that SRCF represents the fraction of clear-sky incoming SW flux falling to the surface which is reflected and absorbed by clouds. Here, SW reflection or absorption by other atmospheric particles such as aerosols is ignored or assumed to be the same for clear and cloudy sky. This non-dimensional quantity offers an effective measure of surface SW cloud forcing and minimizes the influence from non-cloud factors such as aerosol or solar zenith angle. Discussions and applications of SRCF can be found in previous papers [e.g., Betts et al., 2006, Betts, 2009; Betts et al., 2009; Betts and Chiu, 2010; Liu et al., 2011].

### 2.3.2 Cloud Albedo

For studying the quantitative relationship between SRCF, cloud fraction, and cloud albedo, Liu et al. [2011] derived an analytical expression

$$\alpha_{cld}^{SRF} = \alpha_r f \quad (6)$$

where $f$ and $\alpha_r$ denote cloud fraction, and cloud albedo. We estimate cloud albedo by applying SRCF and cloud-fraction data into Equation (6).

### 2.3.3 Procedures of Evaluation

Detailed procedures of the evaluation are described below. First, the 15-min all-sky/clear-sky surface downwelling SW flux and cloud fraction observations are averaged into hourly data. Here, only those with 4 valid 15-min datapoints within one hour are used. The valid 15-min datapoints refer to those with 15-min all-sky/clear-sky surface downwelling SW flux greater than zero and 15-min cloud fraction between 0 and 1. We use the hourly data to calculate the mean value of hourly all-sky/clear-sky surface downwelling SW flux (or cloud fraction) at each season (Spring: March to May, Summer: June to August, Fall: September to November, Winter: December to February). The mean value of hourly SRCF at each season is calculated using the mean value of hourly all-sky/clear-sky surface downwelling SW flux. The mean value of the overall hourly SRCF (or cloud fraction) is the average of the mean values at four seasons. The mean value of overall hourly cloud albedo is calculated using the mean value of overall hourly SRCF (or cloud fraction). Further, those valid hourly all-sky/clear-sky surface downwelling SW flux and cloud fraction between 6am and 6pm (local standard time: LST) are averaged into daytime-mean data. Daytime-mean SRCF is calculated using daytime-mean all-sky/clear-sky surface downwelling SW flux, and daytime-mean cloud albedo is calculated using daytime-mean SRCF and cloud fraction for those with cloud fraction greater than 0.05. Those daytime-mean SRCF (>-0.05) and cloud fraction are further averaged into monthly data. The monthly cloud albedo is calculated by using monthly SRCF and cloud fraction. The mean values of monthly cloud properties at each month and the yearly cloud properties are the averages of the monthly cloud properties.

Next, the cloud properties from hourly ERA-Interim and 6-hourly Reanalysis I/ II are used to calculate the mean values of daytime hourly/6-hourly cloud properties. The calculation procedures

are the same as for the observations. Here, only those hourly/6-hourly reanalysis data concurrent to those valid hourly observations are used. The concurrent 6-hourly reanalysis data refer to those: within those concurrent 6 hours the hourly observations have valid data. Further, those concurrent hourly/6-hourly reanalyses are averaged into daytime-mean, and then those daytime-mean reanalysis data concurrent to those valid daytime-mean observations are averaged into monthly data. The yearly data are the averages of monthly data. The diurnal/monthly/yearly cloud properties from the reanalyses are then evaluated based on the observations.

After that, for diagnosing the path of model-error propagation, the model biases (model minus observation) of the cloud properties and their links are analyzed. We first average the observed 30-min 2m air temperature and relative humidity into hourly data. Then, those concurrent valid hourly data of the observed cloud properties, temperature, and relative humidity are further averaged into daytime-mean and then monthly data. Then, the three reanalyses' hourly/6-hourly cloud properties, 2m air temperature and near-surface relative humidity (only those concurrent to the valid hourly observations) are averaged into daytime-mean and then monthly data. After that, the daytime-mean and monthly model biases of the cloud properties, 2m air temperature and near-surface relative humidity are examined.

Finally, for evaluating the overall performance of the reanalyses in modeling the cloud properties, we employ the widely used technique of the Taylor diagram [Taylor, 2001], and also develop a new metric "Relative Euclidean Distance".

A Taylor diagram reveals concise and easy-to-visual second-order statistical differences between two (or more) different time series. It is especially useful for evaluating a model's performance in phase and amplitude of variations (represented by "correlation" $r$ and "standard

deviation" $\sigma$), and a model's "centered root-mean-square error" $E$ ("RMS error" hereafter). This technique has been widely used in climate researches and IPCC assessment [e.g., IPCC, 2001; Anderson et al., 2004; Martin et al., 2006; Miller et al., 2006; Bosilovich et al., 2008; Gleckler et al., 2008; Pincus et al., 2008]. Briefly, the expressions for calculating $r$, $\sigma$, and $E$ are shown below [Taylor, 2001],

$$r = \frac{\frac{1}{N}\sum_{n=1}^{N}\left(M_n - \overline{M}\right)\left(O_n - \overline{O}\right)}{\sigma_{\mathrm{M}}\sigma_{\mathrm{O}}} \tag{7}$$

$$E^2 = \frac{1}{N}\sum_{n=1}^{N}\left[\left(M_n - \overline{M}\right) - \left(O_n - \overline{O}\right)\right]^2 \tag{8}$$

$$\sigma_M^2 = \frac{1}{N}\sum_{n=1}^{N}\left(M_n - \overline{M}\right)^2 \tag{9}$$

$$\sigma_O^2 = \frac{1}{N}\sum_{n=1}^{N}\left(O_n - \overline{O}\right)^2 \tag{10}$$

with

$$\overline{M} = \frac{1}{N}\sum_{n=1}^{N} M_n \tag{11}$$

$$\overline{O} = \frac{1}{N}\sum_{n=1}^{N} O_n \tag{12}$$

where "$M_n$" or "$O_n$" denote a modeled or observational-based variable, defined at $N$ discrete temporal (or spatial) points; and the subscript "M" or "O" denote a model or observations. Note

that, the "correlation" $r$, "standard deviation" $\sigma$, and "RMS error" $E$ are calculated without removing periodic signals of the variations.

As a supplement to the Taylor diagram, we develop a new metric "Relative Euclidean Distance" ( D ), based on Euclidean-Distance technique (e.g., Elmore and Richman, 2001) and first- and second -order statistics,

$$\mathrm{D} = \sqrt{\left[\frac{\left(\overline{M} - \overline{O}\right)}{\overline{O}}\right]^2 + \left[\frac{(\sigma_{\mathrm{M}} - \sigma_{\mathrm{O}})}{\sigma_{\mathrm{O}}}\right]^2 + (1 - r)^2} \qquad (13)$$

As can be seen from the expression (13), the value of $\mathrm{D}$ gives an overall measure of the model biases from the mean and phase/amplitude of modeled variations. For a perfect agreement, $\mathrm{D} = 0$. The model performance degrades as $\mathrm{D}$ increases.

**3. Evaluation of multiscale cloud properties**

This section evaluates the cloud properties (i.e., SRCF, cloud fraction, and cloud albedo) from the reanalyses. The cloud properties evaluated are at diurnal, annual, and inter-annual temporal scales.

Figure 2 shows the multiscale variations of SRCF from the reanalyses and the observations (upper panels), and corresponding relative model biases [i.e., (model minus observation) divided by observation] (lower panels). Red, blue, green, and purple represent the observations, ERA-Interim, R1, and R2, respectively. Left, middle and right panels represent diurnal, annual and inter-annual variations, respectively. It is evident that the SRCF from the observations and ERA-Interim has a strong annual cycle, with amplitude about 0.15 for the observations and about 0.10 for ERA-Interim. The SRCF peaks in March and reaches its lowest value in July. Both R1 and R2 show a relatively

weaker annual cycle with amplitude about 0.05. R2 (R1) shows a similar (opposite) phase pattern to the observations and ERA-Interim. The diurnal and inter-annual variations of SRCF are weaker than the annual cycle, with amplitude ranging from 0.03 to 0.05. For the diurnal cycle, the observations and R2 show a similar phase pattern with larger (smaller) value in the morning (afternoon), opposite to ERA-Interim and R1. For the inter-annual variations, SRCF reveals a significant drop in 1999 and 2006, especially for the observations and ERA-Interim. One notable phenomenon is that the magnitude of the observed SRCF variations is much larger than that of the reanalyses. In other words, the reanalyses significantly underestimate the observed SRCF. This fact can also be seen from the lower panels, where the relative biases range from -30% to -50% for the majority.

Similar to Figure 2, Figure 3 (or 4) shows the comparison of the multiscale variations of cloud fraction (or cloud albedo). As shown in Figure 3, the multiscale variations of cloud fraction look remarkably similar to those of SRCF, with a strong annual cycle (amplitude up to 0.22) and relatively weak diurnal and inter-annual variations (amplitude up to 0.09). The phase patterns of the multiscale variations of cloud fraction in general follow those of SRCF, suggesting that larger cloud fraction in general corresponds to larger SRCF or vice versa. The underestimation of the modeled cloud fraction is also significant, ranging from -20% to 40% for the majority. Figure 4 reveals a strong annual cycle (amplitude up to 0.20) and slightly weak diurnal and inter-annual variations (amplitude up to 0.15) for the modeled and observed cloud albedo. The phase patterns of the multiscale variations of cloud albedo mainly follow those of SRCF or cloud fraction, except for the annual cycle of the modeled cloud albedo which has the lowest value in winter time, opposite to other annual-cycle patterns. For all the models the underestimation of cloud albedo is small from May to September, but increases to -25% to -30% in the cold season.

## 4. Model biases and their links

The previous section shows that, except for warm season cloud albedo, the three reanalyses significantly underestimate the three cloud properties. To explore further the propagation path for the model errors, this section examines the range of the model biases in the three cloud properties and their links to one another. Also examined is the relationship of the cloud-property biases to the model biases of near-surface temperature and relative humidity, since the cloud properties are known closely related to model-resolved meteorological conditions. The analysis using concurrent daytime-mean and monthly data showed similar conclusions, so we only show the monthly results to illustrate our findings.

Figure 5 are the contour plots showing the range and relationship of the monthly model biases between the cloud properties. Left, middle and right panels represent ERA-Interim, R1 and R2, respectively. As can be seen, the model biases of the cloud properties mainly fall within a centered region, ranging from -0.20 to 0 for SRCF and cloud fraction and from -0.20 to 0.10 for cloud albedo. The intensive points of the model biases exhibit a positive linear relationship to one another, except for the model biases of ERA-Interim cloud fraction and SRCF. The positive correlations are evident in the corresponding scatter plots (Figure 6) as well, where blue, green, and purple represent ERA-Interim, R1, and R2, respectively.

Figure 7 are the scatter plots showing the relationships of the monthly model biases between the cloud properties and near-surface relative humidity and temperature. Blue, green, and purple represent ERA-Interim, R1 and R2, respectively. As can be seen, ERA-Interim has a dry warm bias while R1/R2 has a moist bias with a wider spread in the temperature bias. The model biases of the cloud properties in general exhibit a weak positive linear relationship to the model biases of near-

surface relative humidity, except for ERA-Interim cloud fraction whose biases does not show a clear relationship with its model biases of relative humidity. ERA-Interim model biases of the SRCF and cloud albedo exhibit a negative linear relationship to the model biases of near-surface temperature, while R1/R2 model biases of the cloud properties do not show a clear relationship with those of near-surface temperature. It is likely that the surface biases in temperature and humidity are anti-correlated in ERA-Interim as in an earlier reanalysis, ERA40 (Betts et al 2006).

**5. Evaluation on the overall performance of the reanalyses**

This section evaluates the overall performance of the reanalyses in modeling the cloud properties. The evaluation is conducted using concurrent daytime-mean or monthly data.

Figure 8 shows the Taylor diagrams of the cloud properties from daytime-mean (left panels) and monthly (right panels) data. Red, blue, green, and purple represent the observations, ERA-Interim, R1, and R2, respectively. The symbols "circle", "triangle", and "square" represent SRCF, cloud fraction, and cloud albedo. The radial distance represents the amplitude of the variations, normalized by the amplitude of the observational-based variations. The cosine of azimuthal angle of each point gives the correlation between the reanalyses and the observations. The distance between each point and the reference point "Obs" represents the RMS error, normalized by the amplitude of the observational-based variations. As this distance approaches to zero, the modeled variations approach the observations.

For daytime-mean data, ERA-Interim exhibits the best performance in modeling the phase of the cloud properties and the magnitude of the SRCF variations, although it slightly overestimates the magnitude of the cloud-fraction/cloud-albedo variations. R2 exhibits the best performance in modeling the magnitude of the cloud-fraction/cloud-albedo variations, although it significantly

underestimates the magnitude of the SRCF variations. R2 shows slightly better phase pattern of the cloud properties than R1. R1 significantly underestimates the magnitude of the cloud properties and also shows the worst phase similarity to the observations. ERA-Interim shows the smallest RMS error of SRCF, and R1 shows the smallest RMS error of cloud fraction (or cloud albedo).

For monthly data, ERA-Interim exhibits the best performance in modeling the phase and magnitude and the smallest RMS error of the cloud properties, even though ERA-Interim's underestimation in modeling SRCF is still significant. R2 slightly overestimates the magnitude of the cloud-albedo variations and significantly underestimates the SRCF and cloud-fraction variations. R1 significantly underestimates all the cloud properties, showing the worst in modeling the phase and magnitude and the largest RMS error of the cloud properties.

Figure 9 further compares the "Relative Euclidean Distance" D values of the reanalyses in modeling the daytime-mean (upper) or monthly (lower) cloud properties. Blue, green, and purple represent ERA-Interim, R1, and R2 respectively. As can be seen, ERA-Interim (R1) has the smallest (largest) D values for all the cloud properties for both daytime-mean and monthly temporal scales, suggesting that ERA-Interim (R1) ranks the best (worst) overall performance in modeling the cloud properties among the reanalyses.

**6. Summary**

This study evaluates three major reanalyses (ERA-Interim, NCEP/NCAR Reanalysis I, NCEP/DOE Reanalysis II) in modeling surface relative shortwave cloud forcing (SRCF), cloud fraction, and cloud albedo. The cloud properties at diurnal, annual, and inter-annual temporal scales from all the reanalyses are first evaluated. Then, the model biases are quantified and their links are examined. The overall performance of the reanalyses in modeling the cloud properties is evaluated

using a combined statistical method (i.e., the technique of Taylor diagrams and a newly developed metric "Relative Euclidean Distance"). Decade-long (1997 to 2008) surface-based continuous ARM VAP over the Southern Great Plains (SGP) Central Facility site are used as a standard for this study.

Results show that the reanalyses significantly underestimate the cloud properties, with relative biases ranging mainly from -30% to -50% for SRCF, from -20% to 40% for cloud fraction, and from -10% to -30% for cloud albedo. The annual cycle of the models' relative biases is substantial. For SRCF, ERA-Interim has a uniform negative bias throughout the year, but R1 and R2 have much reduced biases in summer. The annual cycles of the cloud-fraction relative biases differ between the three reanalyses. But for the derived cloud albedo, all the models show a small bias from May to September, increasing in the cold season to a large negative bias of -25% to -30%.

The model biases of the cloud properties predominantly range from -0.20 to 0 for SRCF and cloud fraction and from -0.20 to 0.10 to cloud albedo. The model biases from the majority exhibit a positive linear relationship to one another, and in general show quasi-linear relationships to the model biases of near-surface relative humidity (and temperature for ERA-Interim). These findings suggest that the model biases of the three cloud properties are closely linked to one another, and that the model biases of near-surface meteorological conditions (especially relative humidity) have a direct impact on the model biases of the cloud properties, likely through parameterization schemes.

A combined statistical method, based on first- and second- order statistics, indicates that ERA-Interim (R1) has the best (worst) overall performance in modeling the cloud properties.

The findings from this study highlight the significant underestimation of the cloud properties over the ARM SGP site in the three major NWP reanalyses, and the model biases of the cloud properties are closely linked to one another and also linked to the model biases of near-surface

meteorological conditions (especially relative humidity). This suggests that caution must be taken when using the reanalyses as a standard (e.g., a substitute of observations) for evaluating climate models. Furthermore, the underestimation of the cloud properties is a crucial issue in climate modeling, since it could substantially influence the estimation of the Earth's surface and atmospheric energy budget, hydrological cycle and general circulation. This issue brings direct attention to a future study on the improvement of the model parameterizations for reducing the model biases of the cloud properties. An effective way to make such an improvement is through the improvement of the model parameterizations relevant to cloud fraction, cloud albedo, and near-surface meteorological conditions (especially relative humidity).

It is noteworthy that the extent of the underestimation shown in this study could be partially impacted by the uncertainty of the observations used, especially the single-point observations of cloud fraction which represents $160^{o}$ field-of-view hemispheric fractional sky cover from the surface [Long et al., 2006]. A systematic investigation on quantifying the uncertainty of cloud fraction observations and on developing new approaches to reduce the observational uncertainty [e.g., Min et al., 2008; Hogan et al., 2009] is needed to discern such potential observational effects.

**Acknowledgment.** This work is supported by the Climate System Modeling (ESM) via the FASTER project (www.bnl.gov/esm). The ARM VAP used are obtained from the ARM website (http://www.arm.gov). AKB is partially supported by NSF Grant AGS-0529797. We thank Dr. Charles N. Long for helpful discussions on the ARM SGP observations. The first author thanks Dr. Karl E. Taylor for useful discussions regarding the technique of Taylor diagrams.

**References**


Anderson, J. L., V. Balaji, A. J. Broccoli et al. (2004), The new GFDL global atmosphere and land model AM2–LM2: Evaluation with prescribed SST simulations, *J. Climate*, *17*, 4641-4673.

Anderson, B. T., G. Salvucci, A. C. Ruane, J. O. Roads, M. Kanamitsu (2008), A new metric for estimating the influence of evaporation on seasonal precipitation rates, *J. Hydrometeor*, *9*, 576–588, doi: 10.1175/2007JHM968.1.

Betts, A. K., and P. Viterbo (2005), Land-surface, boundary layer and cloud-field coupling over the south-western Amazon in ERA-40, *J Geophys Res*, *110*, D14108, doi: 10.1029/2004JD005702.

Betts, A.K., J. Ball, A. Barr, T. A. Black, J. H. McCaughey and P. Viterbo (2006), Assessing land-surface-atmosphere coupling in the ERA-40 reanalysis with boreal forest data. *Agricultural and Forest Meteorology, 140*, 355–382, doi:10.1016/j.agrformet.2006.08.009.

Betts, Alan K. (2009), Land-surface-atmosphere coupling in observations and models, *J Adv Model Earth Syst*, **1**, art. #4, 18pp., doi: 10.3894/JAMES.2009.1.4.

Betts, A. K., M. Köhler, and Y. Zhang (2009), Comparison of river basin hydrometeorology in ERA-Interim and ERA-40 reanalyses with observations, *J Geophys Res*, *114*, D02101, doi:10.1029/2008JD010761.

Betts, A. K., and J. C. Chiu (2010), Idealized model for changes in equilibrium temperature, mixed layer depth, and boundary layer cloud over land in a doubled CO2 climate, *J. Geophys. Res.*, *115*, D19108, doi:10.1029/2009JD012888.

Bosilovich, Michael G., Junye Chen, Franklin R. Robertson, and Robert F. Adler (2008), Evaluation of global precipitation in reanalyses, *J Appl Met Clim*, *47*, 2279-2299.

Berrisford, P., D. Dee, K. Fielding, M. Fuentes, P. Kallberg, S. Kobayashi and S. Uppala (2009), The ERA-Interim archive. August 2009. (http://www.ecmwf.int/publications/library/do/references/list/782009)

Dee, D. P., E. Källén, A. J. Simmons, L. Haimberger (2011), Comments on "Reanalyses Suitable for Characterizing Long-Term Trends". *Bull. Amer. Meteor. Soc.*, *92*, 65–70. doi: 10.1175/2010BAMS3070.1.

Elmore, Kimberly L., Michael B. Richman (2001), Euclidean Distance as a Similarity Metric for Principal Component Analysis. *Mon. Wea. Rev.*, *129*, 540–549. doi: 10.1175/1520-0493(2001)129<0540:EDAASM>2.0.CO;2.

Gleckler, P. J., K. E. Taylor, and C. Doutriaux (2008), Performance metrics for climate models, *J Geophys Res*, *113*, D06104.

Haimberger, Leopold, Christina Tavolato, Stefan Sperka (2008), Toward Elimination of the Warm Bias in Historic Radiosonde Temperature Records—Some New Results from a Comprehensive Intercomparison of Upper-Air Data. *J. Climate*, *21*, 4587–4606. doi: 10.1175/2008JCLI1929.1.

Hogan R. J., E. J. O'Connor and A. J. Illingworth (2009), Verification of cloud-fraction forecasts, *Q. J. R. Meteorol. Soc. 135*, 1494–1511, DOI: 10.1002/qj.481.

Intergovenmental Panel on Climate Change (IPCC) (2001), *Climate Change 2001: The Scientific Basis, Contribution of Working Group I to the Third Assessment Report of the Intergovernmental Panel on Climate Change,* edited by J.T. Houghton et al., Cambridge University Press, Cambridge, United Kingdom and New York, NY, USA, 881 pp. (see http://www.grida.no/climate/ipcc_tar/wg1/317.htm#fig84)

Intergovenmental Panel on Climate Change (IPCC) (2007), *Climate Change 2007: The Physical Science Basis*, edited by S. Solomon et al., Cambridge University Press, New York.

Kalnay, E., M. Kanamitsu, R. Kistler et al. (1996), The NCEP/NCAR 40-year reanalysis project. *Bull. Amer. Meteor. Soc., 77*, 437–471.

Kanamitsu, M., W. Ebisuzaki, J. Woollen, S.-K. Yang, J. J. Hnilo, M. Florino, and G. L. Potter (2002), NCEP–DOE AMIP–II reanalysis (R-2). *Bull. Amer. Meteor. Soc., 83,* 1631–1643.

Kassianov, E., C. N. Long, and M. Ovtchinnikov (2005), Cloud sky cover versus cloud fraction: Whole-sky simulations and observations, *J. Appl. Meteorol., 44*, 86–98, doi:10.1175/JAM-2184.1.

Kistler, R., and Coauthors (2001), The NCEP–NCAR 50-year reanalysis: Monthly means CD-ROM and documentation. *Bull. Amer. Meteor. Soc., 82,* 247–267.

Liu, Y., W. Wu, M. P. Jensen, and T. Toto (2011), Relationship between cloud radiative forcing, cloud fraction and cloud albedo, and new surface-based approach for determining cloud albedo, *Atmos. Chem. Phys., 11*, 7155-7170, doi:10.5194/acp-11-7155-2011.

Long, C. N. and T. P. Ackerman (2000), Identification of Clear Skies from Broadband Pyranometer Measurements and Calculation of Downwelling Shortwave Cloud Effects, *J. Geophys. Res.* , *105*, No. D12 (2000), pp. 15609-15626.

Long, C. N., T. P. Ackerman, K. L. Gaustad, and J. N. S. Cole (2006), Estimation of fractional sky cover from broadband shortwave radiometer measurements*, J. Geophys. Res., 111,* D11204, doi:10.1029/2005JD006475.

Lu, Cheng-Hsuan, Masao Kanamitsu, John O. Roads, Wesley Ebisuzaki, Kenneth E. Mitchell, Dag Lohmann (2005), Evaluation of soil moisture in the NCEP–NCAR and NCEP–DOE global reanalyses. *J. Hydrometeor*, *6*, 391–408. doi: 10.1175/JHM427.1.

Martin, G. M., M. A. Ringer, V. D. Pope, A. Jones, C. Dearden, and T. J. Hinton (2006), The physical properties of the atmosphere in the new Hadley Centre Global Environmental Model (HadGEM1). Part I: model description and global climatology, *J Climate*, *19*, 1274-1301.

Miller, R. L., G. A. Schmidt, and D. T. Shindell (2006), Forced annular variations in the 20th century Intergovernmental Panel on Climate Change Fourth Assessment Report models, *J Geophys Res*, *111*, D18101.

Min, Q., T. Wang, C. N. Long, and M. Duan (2008), Estimating fractional sky cover from spectral measurements*, J. Geophys. Res., 113*, D20208, 6 PP., doi:10.1029/2008JD010278.

Peixoto, J. P., A. H. Oort (1992), *Physics of Climate*, 520pp, Springer-Verlag New York Inc., New York.

Pincus, R., C. P. Batstone, R. J. P. Hofmann, K. E. Taylor, and P. J. Glecker (2008), Evaluating the present-day simulation of clouds, precipitation, and radiation in climate models, *J Geophys Res*, *113*, D14209.

Rye, Cameron J., Neil S. Arnold, Ian C. Willis, and Jack Kohler (2010), Modeling the surface mass balance of a high Arctic glacier using the ERA-40 reanalysis, *J Geophys Res*, *115*, F02014.

Simmons, A. J., K. M. Willett, P. D. Jones, P. W. Thorne, and D. P. Dee (2010), Low-frequency variations in surface atmospheric humidity, temperature and precipitation: Inferences from reanalyses and monthly gridded observational datasets. *J. Geophys. Res.*, 115, D01110, doi:10.1029/2009JD012442.

Taylor, K. E. (2001), Summarizing multiple aspects of model performance in a single diagram, *J. Geophys. Res.*, *106*, 7183-7192.

Thorne, P. W., and R. S. Vose (2010) Reanalyses suitable for characterizing long-term trends: Are they really achievable? *Bull. Amer. Meteor. Soc., 91***,** 353–361.

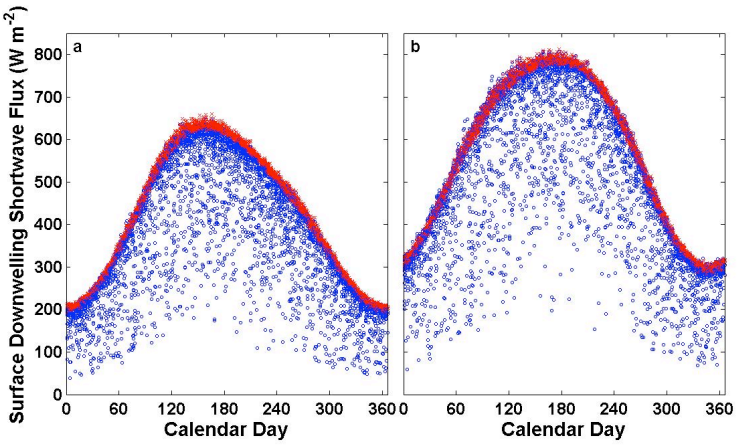


Figure 1. Annual distribution of R2 6-hourly (a. 6am-12pm LST; b. 12pm-6pm LST) surface downwelling shortwave flux over the ARM SGP Central Facility site from 03/25/1997 to 12/31/2008. The symbol "x" (red) represents R2 clear-sky surface downwelling shortwave flux, estimated by using R1 clear-sky surface downwelling shortwave flux. The symbol "o" (blue) represents available R2 all-sky surface downwelling shortwave flux.

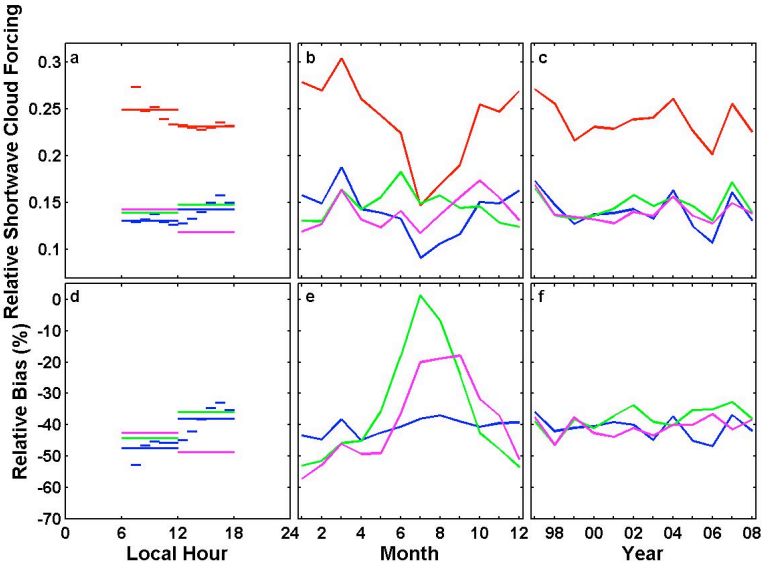


Figure 2. Multiscale variations of surface relative shortwave cloud fraction (SRCF) (a, b, c) and corresponding relative model biases (d, e, f), defined as [(model minus observation) divided by observation]. Red, blue, green, and purple represent the observations, ERA-Interim, R1, and R2, respectively. The data used are daytime (6am to 6pm LST) data from 03/25/1997 to 12/31/2008 over ARM SGP Central Facility site.

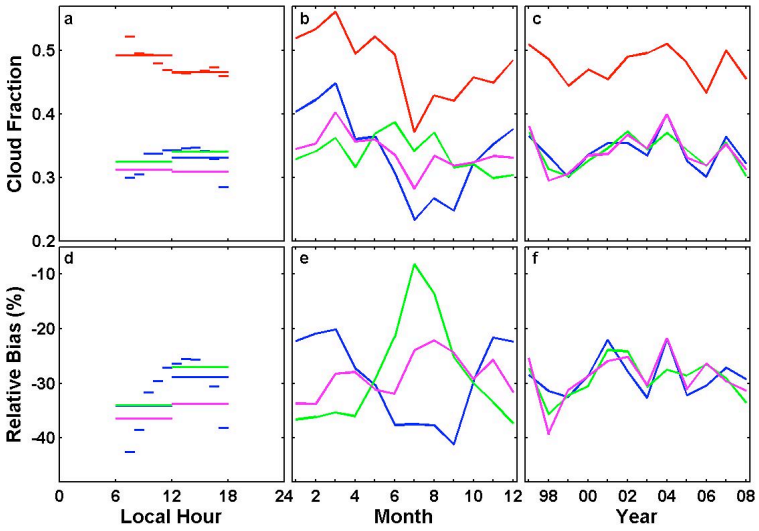


Figure 3. The same as Figure 2, except that this figure is about cloud fraction instead of surface relative shortwave cloud fraction (SRCF).

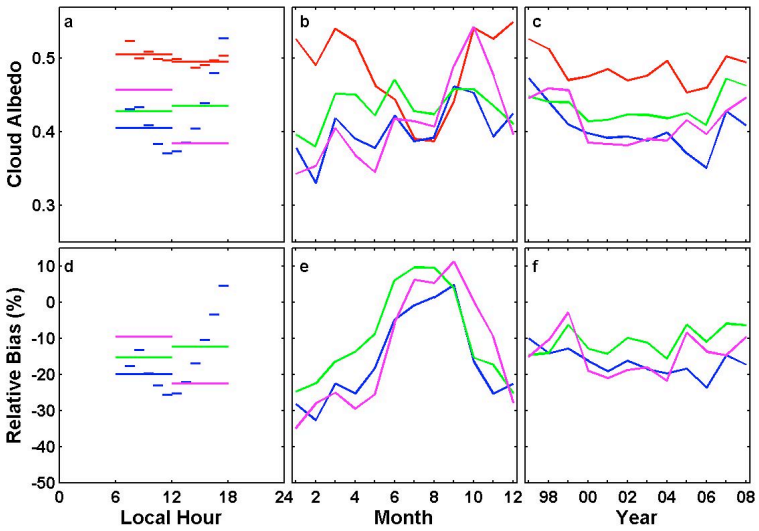


Figure 4. The same as Figure 2, except that this figure is about cloud albedo instead of surface relative shortwave cloud fraction (SRCF).

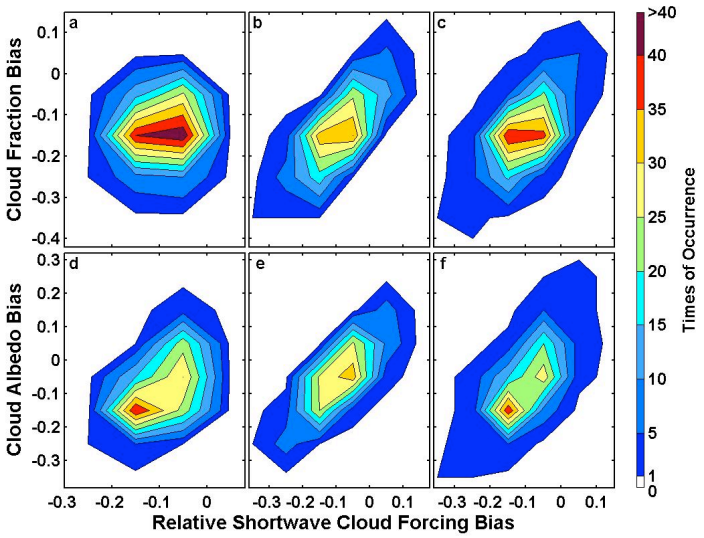


Figure 5. Contour plots showing the range and relationship of the monthly model biases between the cloud properties. Left (a, d), middle (b, e) and right (c, f) panels represent ERA-Interim, R1 and R2, respectively.

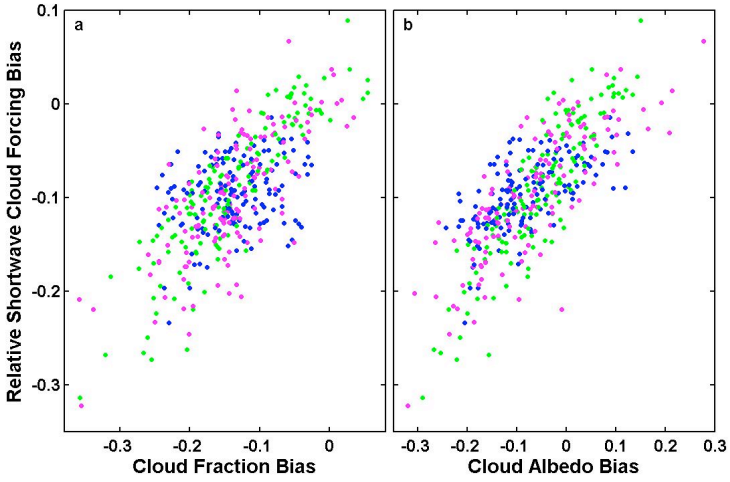


Figures 6. Scatter plots showing the relationship of the monthly model biases between the cloud properties. Blue, green, and purple represent ERA-Interim, R1, and R2, respectively.

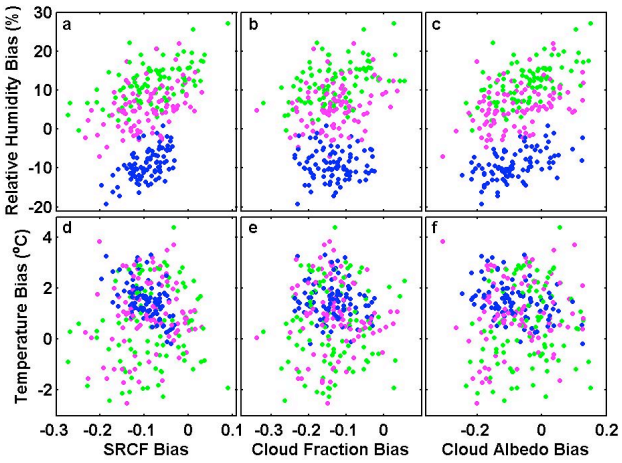


Figure 7. Scatter plots showing the relationships of the monthly model biases between the cloud properties and near-surface relative humidity (or temperature). Blue, green, and purple represent ERA-Interim, R1, and R2, respectively. "SRCF" denotes surface relative shortwave cloud fraction as in the text.

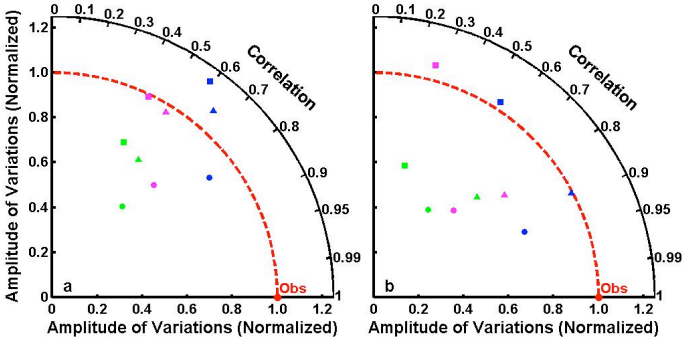


Figure 8. Taylor diagrams of the cloud properties from daytime-mean (left) or monthly (right) data. Red, blue, green, and purple represent the observations, ERA-Interim, R1, and R2, respectively. The symbols "circle", "triangle", and "square" represent surface relative shortwave cloud fraction (SRCF), cloud fraction, and cloud albedo.

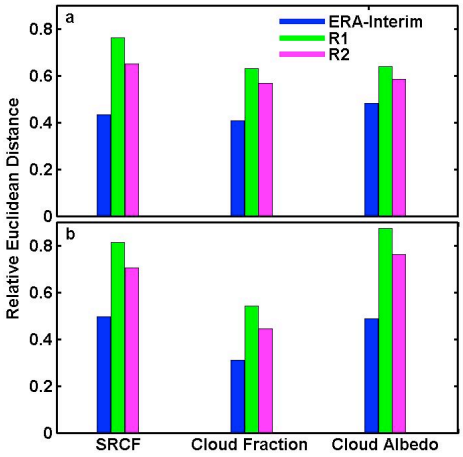


Figure 9. "Relative Euclidean Distance" of the cloud properties from daytime-mean (upper) and monthly (lower) data. "SRCF" denotes surface relative shortwave cloud fraction as in the text. The shorter the distance, the better a model's performance is.